

## RECONFIGURATION IN THE ATTITUDE CONTROL OF ICOSAHEDRAL BODIES

JIŘÍ BENEŠ

Specific polyhedral diagrams of angular velocity distributions, resulting from triplets of component vectors pointing to the midpoints of faces of a regular icosahedral body in space and generated by auxiliary driving means are described. The distributions of the number of these triplets as functions of the module and argument of the resulting vector are introduced. A map of the "firmament" for an observer placed in the centre of the icosahedral body is given, showing the attainable end-points of the resulting angular velocity vectors. Examples of reconfiguration are deduced from this map which is intended as a part of the information pattern of the computer for attitude control in space.

The attitude control of an icosahedral body in space, using a controlling moment, which effects its rotation e.g. around the Euler axis as in the case of extensive control [1], is assumed by computer controlled application of appropriately selected triplets of component angular velocity vectors, generated by auxiliary driving means. By summing up these triplets taken as combinations by three from a set of 20 component vectors, different resulting angular velocity vectors are obtained, the end-points of which are considered as vertices of a three-dimensional graph: the polyhedral diagram of angular velocity distribution [2]. If any active auxiliary driving means falls out, this can be remedied: 1) by generating instead promptly another triplet, having the same sum as the previous one before its defection (if this is possible, as for diagram vertices, obtainable in two or three ways); 2) by selecting appropriate triplets of vectors, corresponding to vertices of another suitable polyhedral diagram, in order to reach a goal in attitude control similar in angular coordinates, but eventually with a smaller module of the resulting angular velocity vector [3]. Both these methods enter into the general concept of reconfiguration embodied in the attitude control system. The described generation of the resultant angular velocity vector and its application are intended primarily for coarse attitude control, the fine control making use of further information from the sensors and of the fine mechanism of control of the auxiliary driving means.

The regular icosahedral body is depicted in the basic system of axes  $x, y, z$  in Fig. 1, where  $z$  points to the reader. The length of its edge is  $a = 100.000000$ , the radius of its circumscribed sphere is  $R_{0i} = 95.105651629$ . The 20 component angular velocity vectors are oriented into the midpoints of the faces of the icosahedron. For

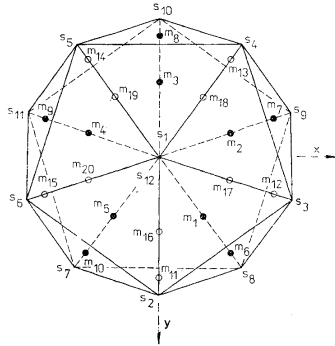


Fig. 1. The regular icosahedron with the midpoints  $m_i$  ( $i = 1, \dots, 20$ ) of its faces.

example, the length coordinates of midpoint  $m_2$  in Fig. 1 are:  $x_2 = 43.633899812$ ,  $y_2 = -14.177513472$ ,  $z_2 = 60.056910821$ . All the component vectors have the same module  $M = 75.5761340$  [the dimension is that of angular velocity, which will not be recalled in the sequel]. By summing them up by three (without excluding pairs of vectors with the opposite sense), one obtains a set of resulting vectors with a number of elements

$$V_m = \binom{30}{3} = 1140.$$

Table 1.

Subset	M	$v_m$	c	e	f	f3	f4	f5	f6	f10	Polyhedral diagram
$I_M$	31-701884	60	12	30	20	20					icosahedron
$II_M$	62-561459	60	60	90	32			12	20		truncated icosahedron
$III_M$	75-576131	220	20	30	12			12			dodecahedron
$IV_M$	92-847608	120	60	120	62	20	30	12			small rhombicosidodecahedron
$V_M$	115-444448	180	60	90	32			12	20		truncated icosahedron
$VI_M$	127-421926	60	60	90	32	20			12		truncated dodecahedron
$VII_M$	134-291335	60	12	20	20	20					icosahedron
$VIII_M$	144-717274	120	120	180	62		30		20	12	great rhombicosidodecahedron
$IX_M$	160-155648	120	60	90	32	20			12		truncated dodecahedron
$X_M$	168-993367	20	20	30	12			12			dodecahedron
$XI_M$	182-388323	60	60	90	32			12	20		truncated icosahedron
$XII_M$	194-864678	60	60	120	62	20	30	12			small rhombicosidodecahedron

This set can be decomposed into 12 subsets according to the module  $M$  of the resulting vector. Table 1 gives the characteristics of the relevant polyhedral diagrams having the end-points of the resulting vectors as vertices. Here,  $M$  is the module of the resulting vectors belonging to the subset,  $v_m$  is the number of combinations in the subset;  $c$  is the number of vertices;  $e$  the number of edges,  $f$  the number of faces;  $f_3, f_4, f_5, f_6, f_{10}$  are numbers of the triangular, quadrilateral, pentagonal, hexagonal, decagonal faces respectively. It is

$$V_m = 1140 = \sum_{m=1}^{12} v_m.$$

The distribution of  $v_m$  as function of  $M$  is in Fig. 2. On its basis, and that of Table 1, three neighboringly united ( $n$ -united, in the sense of [2]) bodies have been constructed:

**CASE A: THE SMALL ICOSICOSODODECAHEDRON**, shown in Fig. 5, resulting from the union of subset  $XI_M$  (set of vertices of the truncated rhombicosahedron in Fig. 3) and of subset  $XII_M$  (set of vertices of the small rhombicosidodecahedron in Fig. 4).

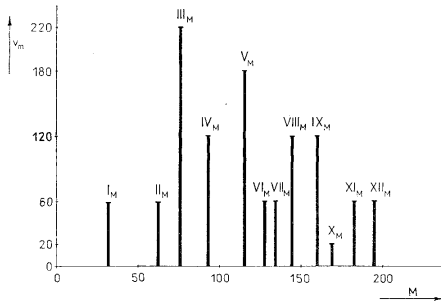


Fig. 2. The distribution of  $v_m$  as function of the module  $M$  of the resulting vector.

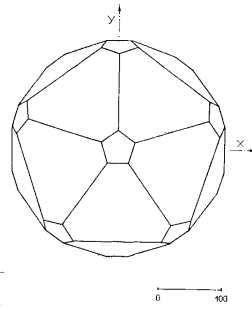


Fig. 3. The truncated icosahedron from subset  $XI_M$ .

**CASE B: THE (3-4-10)-HECATONPENENTADIOHEDRON**, shown in Fig. 8, resulting from the union of subset  $VIII_M$  (set of vertices of the great rhombicosidodecahedron in Fig. 6) and of subset  $IX_M$  (set of vertices of the truncated dodecahedron in Fig. 7).

**CASE C: THE (3-4-5)-HECATONPENENTADIOHEDRON**, shown in Fig. 11, resulting from the union of subset  $V_M$  (set of vertices of the truncated icosahedron in Fig. 9) and of subset  $VI_M$  (set of vertices of the truncated dodecahedron in Fig. 10).

The characteristics of the three bodies (for case A, B, C) are given in Table 2. Here,

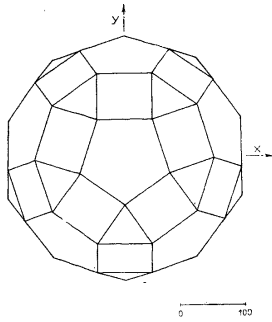


Fig. 4. The small rhombicosidodecahedron from subset XII<sub>M</sub>.

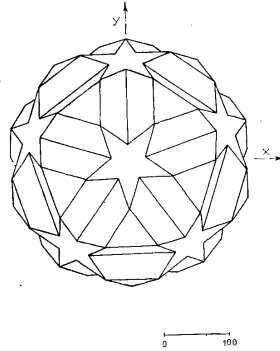


Fig. 5. The small icosicosododecahedron.

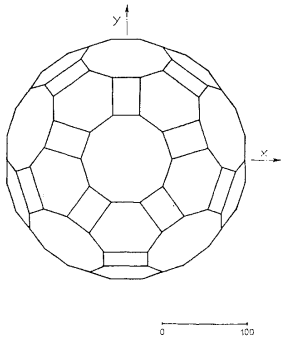


Fig. 6. The great rhombicosidodecahedron from subset VIII<sub>M</sub>.

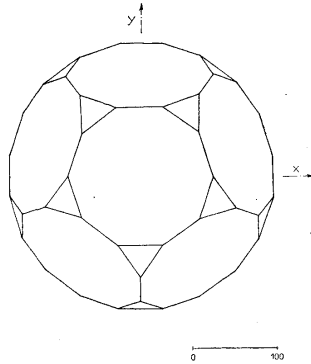


Fig. 7. The truncated dodecahedron from subset IX<sub>M</sub>.

$\overline{\overline{M}}$  denotes the mean square value of the radius of the representative sphere of the  $n$ -united polyhedral diagram and  $\delta_1$  and  $\delta_2$  express the quality of approximating the representative sphere by the  $n$ -united polyhedral diagram. For case A:

$$\overline{\overline{M}} = \left( \frac{60 \cdot 194 \cdot 864678^2 + 60 \cdot 182 \cdot 388323^2}{120} \right)^{\frac{1}{2}} = 188 \cdot 729625521,$$

$$\delta_1 = 194 \cdot 864678 : 188 \cdot 729625521 = 1 \cdot 032507098,$$

$$\delta_2 = 182 \cdot 388323 : 188 \cdot 729625521 = 0 \cdot 966400068.$$

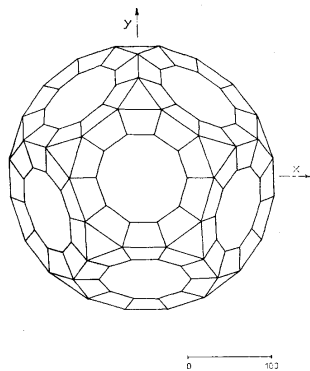


Fig. 8. The (3-4-10)-hecatonpentadiohedron.

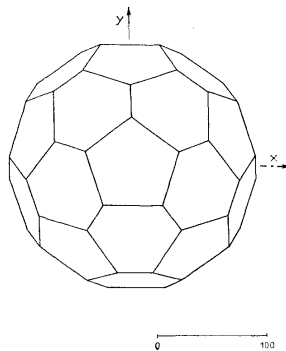


Fig. 9. The truncated icosahedron from subset  $V_M$ .

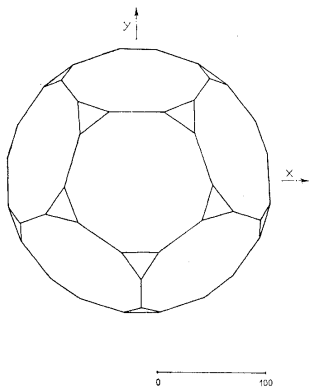


Fig. 10. The truncated dodecahedron from subset  $VI_M$ .

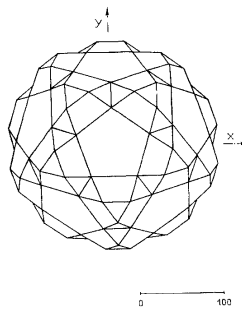


Fig. 11. The (3-4-5)-hecatonpentadiohedron.

The distribution of the number of combinations  $v_m$  as a function of the module  $M$ , as in Fig. 2, has proved valuable for the selection and purposeful formation of new polyhedral diagrams [3]. Following a personal suggestion [4], a distribution of the set of combinations as a function of the argument of the resulting vector has been investigated.

Let  $\varphi$  be the angle between the resulting angular velocity vector and the  $z$  axis of the basic system. The decomposition of the set of the 1140 resulting vectors accord-

Table 2.

Case	Fig.	Body	$\bar{M}$	$\delta_1$	$\delta_2$	c	e	f	f3	f4	f5	f10
A	5	SMALL ICOSICOSO-DODECAHEDRON	188-729625521	1-032507098	0-966400068	120	210	92	20	60	12	
B	8	(3-4-10)-HECATON-PENENTADIOHEDRON	150-040006191	1-067419630	0-964524580	180	330	152	20	120	12	
C	11	(3-4-5)-HECATON-PENENTADIOHEDRON	121-580771093	1-048043410	0-949528835	120	270	152	80	60	12	

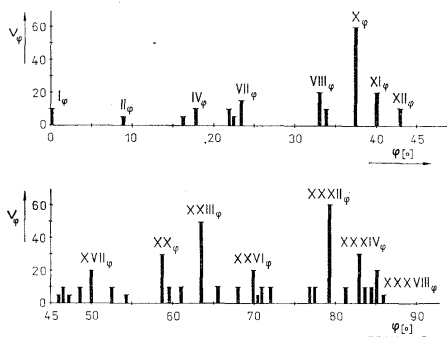


Fig. 12. The distribution of  $v_\varphi$  as function of the angle  $\varphi$  for the range 0 to  $\pi/2$  (left above: for 0 to  $\pi/4$ , left below: for  $\pi/4$  to  $\pi/2$ ).

ing to discrete values of  $\cos \varphi$  some of which are positive and others negative, yields 76 subsets. Being interested here for brevity mainly in the upper part (hemisphere) of the diagram, we consider only positive values of  $\cos \varphi$  and arrange the respective 38 subsets in the order of increasing values of  $\varphi$  from  $0^\circ$  to  $90^\circ$ . The distribution is in Fig. 12. For brevity we give the characteristics of some of the subsets only:

Subset	$\varphi^0$	M	$v_\varphi$
$I_\varphi$	0-00000000	31-701884	10
$II_\varphi$	8-943913546	182-388323	5
$\vdots$	$\vdots$	$\vdots$	$\vdots$
$XXXVII_\varphi$	84-921357944	160-155648	20
$XXXVIII_\varphi$	85-827701764	194-864678	5

It is

$$V_\varphi = 2 \sum_{\varphi=1}^{38} v_\varphi = 2 \cdot 570 = 1140.$$

Let us now investigate more closely the vertices contained in the octant given by the positive values of the coordinates  $x, y, z$  and belonging to the polyhedral diagrams of cases A, B, C (Fig. 5, 8 and 11). Let  $\beta$  be the angle between the projection of the resulting angular velocity vector into the plane  $xy$  and the  $x$  axis of the basic system. Let  $\alpha = (\pi/2) - \varphi$ . The set of the vertices of the three polyhedrons of Table 2, belonging to the octant  $xyz$ , is represented in the angular coordinates  $\beta, \alpha$  in Fig. 13, where full dots stem from case A, half-full dots from case B and empty dots from case C. Let us remark that this figure gives the angular coordinates of the bodies (vertices) in the  $xyz$  quadrant of a "firmament" for a hypothetical observer at the origin of the basic system  $x, y, z$ , seated towards  $Ox$ , with  $Oy$  at his left and  $Oz$  pointing overhead (to the "zenith"), the "horizon" being in the plane  $xy$ . Correlating these points with the respective triplets of component angular velocity vectors, a set of rules can be established which may be useful for the algorithmic resources (including the information pattern) of the computer (the formator) used both for control and reconfiguration. For the octant considered an auxiliary diagram of the deployed part of the icosahedron (with face 1 at its centre) may be used as in Fig. 14. The rules may be stated e.g. as follows: (Fig. 13):

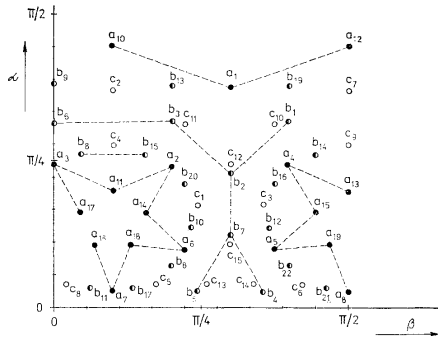


Fig. 13. The map of the "firmament" for a hypothetical observer at the centre of the icosahedral body (in angular coordinates  $\alpha, \beta$ ).

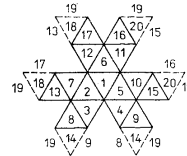


Fig. 14. The auxiliary diagram with face 1 at its centre.

"The points of the right star are attainable by combinations by three of the vectors aiming to the midpoints of the faces of the prismatic roof 1-2-7-12-6".

"Those of the left star by combinations by three of the vectors aiming to the faces of the prismatic roof 1-6-11-10-5".

"The remaining full points are attainable by combinations by three of the vectors aiming to the faces of the prismatic roof 1-5-4-3-2"; etc.

There are interesting symmetry relations which appear when marking the triplets of component vectors on the auxiliary diagram of Fig. 14.

In order to indicate the possibilities of the reconfiguration, let us concentrate upon a central portion of Fig. 13 as redrawn in Fig. 15 with the indication by concentric circles

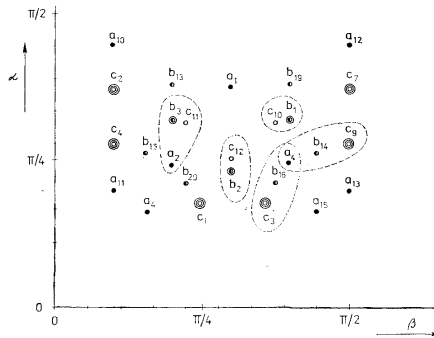


Fig. 15. The central portion of the map of Fig. 13 with indication by concentric circles of vertices attainable by 2 or 3 triplets.

circles of those vertices which can be attained by two, resp. three triplets of component vectors. The vertices can be reached by these triplets:

A) Full dot vertices (Case A):

$a_1$	1 - 2 - 5	$a_{12}$	1 - 3 - 5
$a_2$	1 - 2 - 6	$a_{13}$	1 - 5 - 11
$a_4$	1 - 5 - 6	$a_{14}$	1 - 6 - 7
$a_{10}$	1 - 2 - 4	$a_{15}$	1 - 6 - 10 ;
$a_{11}$	1 - 2 - 12		

B) Half-full dot vertices (Case B):

$b_1$	1 - 2 - 10 or 1 - 4 - 6		
$b_2$	1 - 2 - 11 or 1 - 5 - 12		
$b_3$	1 - 3 - 6 or 1 - 5 - 7		
$b_{13}$	2 - 4 - 6	$b_{16}$	2 - 6 - 10
$b_{14}$	2 - 5 - 11	$b_{19}$	3 - 5 - 6
$b_{15}$	2 - 5 - 12	$b_{20}$	5 - 6 - 7



C) Empty dot vertices (Case C):

- $c_1$  1 - 2 - 16 or 2 - 10 - 12 or 4 - 6 - 12
- $c_2$  1 - 5 - 13 or 2 - 3 - 11 or 3 - 5 - 12
- $c_3$  1 - 5 - 17 or 3 - 6 - 11 or 5 - 7 - 11
- $c_4$  1 - 6 - 8 or 2 - 7 - 10 or 4 - 6 - 7
- $c_7$  1 - 2 - 15 or 2 - 4 - 11 or 4 - 5 - 12
- $c_9$  1 - 6 - 9 or 3 - 6 - 10 or 5 - 7 - 10
- $c_{10}$  1 - 3 - 11
- $c_{11}$  1 - 4 - 12
- $c_{12}$  1 - 7 - 10.

Some of the subsets of vertices, which may be considered for the purpose of re-configuration, are encompassed by bundles in Fig. 15.

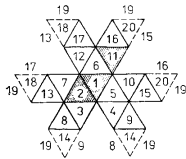


Fig. 16. Symmetry of triplets 1-2-11 and 1-5-12 shown on the auxiliary diagram.

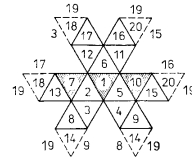
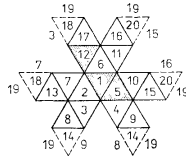


Fig. 17. Triplet 1-7-10 for attaining vertex  $c_{12}$  in the second stage of reconfiguration.

As an example, let us consider the vertex  $b_2$  (case B) from the point of view of the reconfiguration. This point is attainable by two triplets of vectors: 1 - 2 - 11 or 1 - 5 - 12. If one of these fails, it can be at first replaced by the other. This is connected with a symmetry, observable on the pertinent auxiliary diagrams of Fig. 16. If both these triplets fail, there is a second stage of reconfiguration possible, connected with the transition to the vertex  $c_{12}$  of the polyhedral diagram for case C, i.e. with a loss in the value of the module of the resultant angular velocity vector from  $M = 160.155648$  to  $M = 127.421926$ . The required triplet is 1 - 7 - 10 represented on the auxiliary diagram of Fig. 17, which can be easily compared with those of Fig. 16.

An other example of reconfiguration can be followed in Fig. 15 as two subsequent transitions: 1) from vertex  $a_2$  (triplet 1 - 2 - 6) to vertex  $b_3$  (triplet 1 - 3 - 6 or 1 - 5 - 7); 2) from vertex  $b_3$  to vertex  $c_{11}$  (triplet 1 - 4 - 12). The whole re-configuration is connected with a loss of the module of the resultant angular velocity vector from  $M = 194.864678$  (point  $a_2$ ) over  $M = 160.155648$  (point  $b_3$ ) to  $M =$

= 127-421926 (point  $c_{11}$ ). The stages of the reconfiguration can be followed on the auxiliary diagrams of Fig. 18. Surprisingly enough, the changes in these diagrams involve neighbouring or near faces, and without previous thorough analysis of the polyhedral diagrams it would be hardly possible to predict their effect.

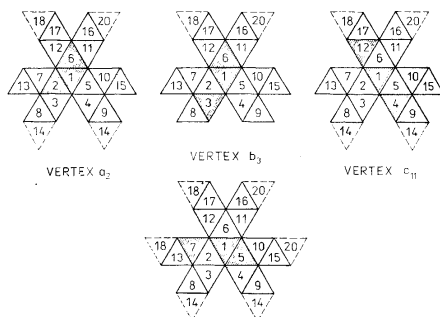


Fig. 18. The stages of reconfiguration from vertex  $a_2$  to vertex  $b_3$  (attainable in two ways) and to vertex  $c_{11}$ .

For purposes of the analysis of the effect of the loss of activity of individual auxiliary driving means and for purposes of subsequent reconfiguration it is advisable to partition the faces of the icosahedron into five subsets and to colour them e.g. in this symmetric way (Fig. 1): red: 5, 7, 14, 16; blue: 3, 10, 12, 19; green: 1, 8, 15, 17; yellow: 2, 9, 11, 18; orange: 4, 6, 13, 20. In the case of specific failures, accordingly impoverished maps from those in Fig. 13 and Fig. 15 can be drawn, with the loss of the pertinent color component in the triplets.

In conclusion let us express the hope that this analysis may be of some interest to those who study the dynamics of icosahedral bodies on different scales and in different disciplines. In Cybernetics the interest in the group of the icosahedron may be justified also e.g. by the intriguing open problems of the morphogenesis of icosahedral viruses and the pertinent deltahedrons with icosahedral symmetry (icosadeltahedrons), where a concurrent application of biochemical and crystallographic approaches may be indicated.

#### ACKNOWLEDGEMENTS

The author wishes to thank Jiří Grim for efficient computational work and Miss Sonja Sovová for drawing the many preparatory and final figures.

(Received February 23, 1983.)

#### REFERENCES

---

- [1] Petrov, B. N., Bodner, V. A., Alekseev, K. B.: Analiticheskoe reshenie zadachi upravleniya prostranstvennym povorotnym manevrom. Doklady AN SSSR 192 (1970), 6, 1235—1238.
- [2] J. Beneš: Polyhedral diagrams of angular velocity distributions in the control of dodecahedral bodies. Problems Control Inform. Theory 8 (1979), 2, 85—103.
- [3] J. Beneš: The shaping and reconfiguration of polyhedral diagrams. In: Fourth Formator Symposium on Mathematical Methods for the Analysis of Large Scale Systems (J. Beneš, L. Bakule, eds.). Academia, Prague 1983, 53—68.
- [4] Personal suggestion from Dr. Otakar Šefl of Prague.
- [5] M. Wenninger: Polyhedron Models. Cambridge University Press, Cambridge 1971.

*Ing. dr. Jiří Beneš, Dr.Sc., Ústav teorie informace a automatizace ČSAV (Institute of Information Theory and Automation — Czechoslovak Academy of Sciences), Pod vodňanskou věží 4, 182 08 Praha 8, Czechoslovakia.*